Volume 13 | Number 6 | June 2014 | Pages 833–972

Photochemical & Photobiological Sciences

An international journal

www.rsc.org/pps

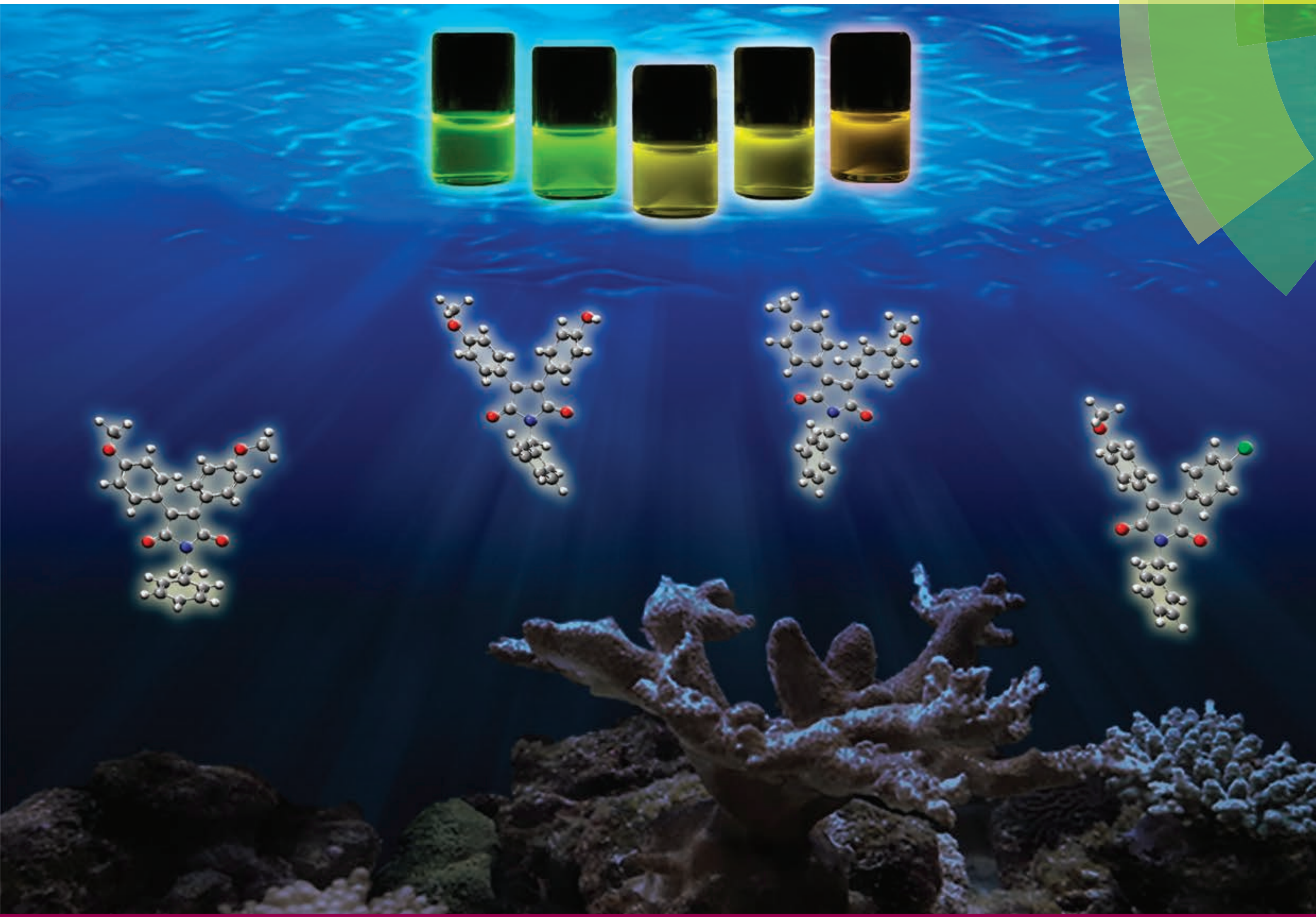

Themed issue: International Conference on Photochemistry 2013 (ICP2013) keynote lectures

ISSN 1474-905X

ROYAL SOCIETY OF CHEMISTRY

Photochemical & Photobiological Sciences

PAPER

Cite this: *Photochem. Photobiol. Sci.*, 2014, **13**, 859

Fluorescence from bisaryl-substituted maleimide derivatives†

Milena Helmer Lauer,[a] Roberta Lopes Drekener,[b] Carlos Roque Duarte Correia[b] and Marcelo Henrique Gehlen*[a]

Received 1st January 2014,
Accepted 29th March 2014

DOI: 10.1039/c4pp00001c

www.rsc.org/pps

A series of bisaryl-substituted fluorescent maleimides was synthesized *via* the Heck arylation. The compounds showed broad fluorescence emission bands in the visible region, a large Stokes shift in polar solvents and emission quantum yields varying from 0.04 to 0.71, depending on the structure and solvent medium. The difference in dipole moments of ground and excited electronic states of about 12 Debye is ascribed to a substantial charge shift and push–pull character of bisaryl-substituted maleimides. The fluorescence decays of *N*-benzyl-3,4-bis(4-methoxyphenyl)-1*H*-pyrrole-2,5-dione (compound **5a**) are biexponential with short (1.3–7.6 ns) and long lived (11.5–13.6 ns) components in polar solvents, but in 1,4-dioxane and THF the decays become single exponential. On the other hand, *N*-benzyl-3-(4-methoxyphenyl)-4-(4-hydroxyphenyl)-1*H*-pyrrole-2,5-dione (compound **5b**) exhibited a biexponential decay in DMSO and in DMF with much shorter decay components, and such behavior indicated a charge shift process combined with solvent assisted proton transfer in the excited state.

1 Introduction

Natural products with intrinsic or derived fluorescence have been used as molecular probes to study biological processes like intracellular trafficking, membrane association and autotoxicity.[1,2] For this purpose, some strategies such as synthesis of fluorescent analogs have been successfully employed.[1–3] Thus, the evaluation of the photochemical stability, quantum yield, and fluorescence lifetime of new fluorophores based on natural products is an important issue for future applications as molecular probes.

A class of compounds used for optical sensing is the aromatic imides. The photophysical properties of monoimides and polyimides are well-documented.[4,5] However, the fluorescent properties of bisaryl-substituted maleimide derivatives have not been fully described, although their natural precursors, polycitrin A and B, isolated from the marine ascidian *Polycitor* sp. by Kashman *et al.*,[6] have been known for many years.

When the fluorophore presents a charge shift character in the excited state, it can be used as a reporter of local polarity in biological systems,[7,8] polymers,[9] and colloids.[10,11] Molecules with the so-called push–pull effect should have well positioned electron-donating and electron-accepting groups linked by a π-conjugated bridge.[12,13] Upon electronic excitation an increase in charge separation may occur, and excited state properties become dependent on the solvent polarity.[14,15]

In this report, photophysical properties of bisarylated maleimides are determined by stationary and time resolved emission spectroscopy. The compounds (see structures **5a–d** in Fig. 1) were synthesized *via* the Heck arylation.[16] Furthermore, to investigate the effect of solvent polarity on energy levels and to determine the difference in dipole moments, the Lippert–Mataga approach was employed.[17,18] Theoretical calculations using density functional theory (DFT) methods at the B3LYP/6-311G++(2d,2p) level were used to evaluate the dipole moment of the ground state of the compounds.

2 Experimental

2.1 Synthesis

2.1.1 Materials and methods. The ^{1}H NMR spectroscopic data were recorded using a Bruker spectrometer at 250 MHz and 500 MHz in $CDCl_3$, $(CD_3)_2CO$, $(CD_3)_2SO$, and CD_3CN solutions. The chemical shifts are reported in ppm and referenced to the residual solvent peak or tetramethylsilane (TMS). The spectroscopic data are reported in the order of chemical shift (*δ*), multiplicity, coupling constant (*J*) in hertz, and integrated intensity. The ^{13}C NMR spectroscopic data were recorded using a Bruker spectrometer at 62.5 MHz and 125 MHz in $CDCl_3$, $(CD_3)_2CO$, $(CD_3)_2SO$, and CD_3CN solutions. The chemi-

---

[a] *Institute of Chemistry of São Carlos, University of São Paulo, CEP 13560-590, São Carlos, SP, Brazil. E-mail: marcelog@iqsc.usp.br; Tel: +55 16 33739928*
[b] *Institute of Chemistry, State University of Campinas, CEP 13083-862, Campinas, SP, Brazil*

† Electronic supplementary information (ESI) available: Optimized geometry of compounds, contribution of dipole moments in each direction, absorption spectra and Lippert–Mataga plots. See DOI: 10.1039/c4pp00001c

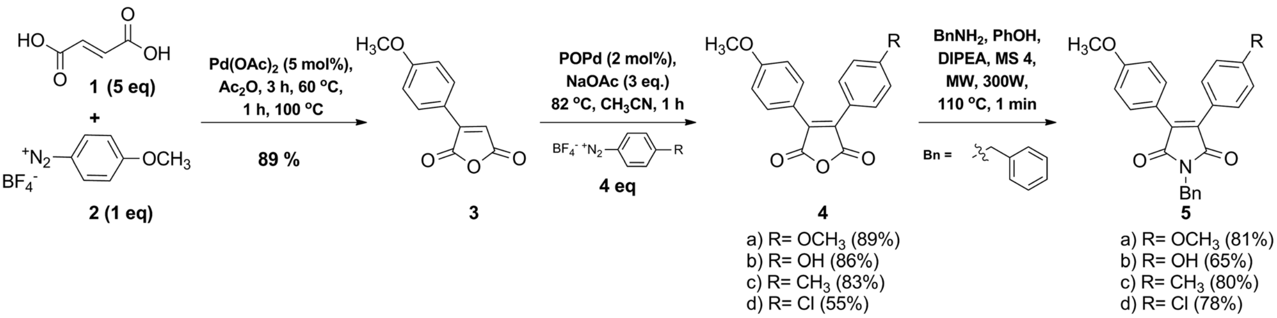

Fig. 1 Reaction scheme of the Heck arylation.

cal shifts are reported in ppm and referenced to the residual solvent peak. For the mass spectroscopy, the compounds were ionized by 70 eV EI and the exact masses were determined with a Waters GCT TOF mass analyzer. The microwave (MW) reactions were conducted in a microwave synthesizer (CEM Discover®) system with a power output of about ≤300 W. These reactions were performed in glass vessels (capacity 10 mL) sealed with a septum. The temperature measurements were conducted with an infrared temperature sensor mounted under the reaction vessel. All of the experiments were performed using a stirring option, whereby the contents of the vessel were stirred by means of both a rotating magnetic plate located below the floor of the microwave cavity and a Teflon-coated magnetic stir bar inside the vessel. The experiments were carried out by simultaneously cooling with compressed air passed through the microwave cavity and heating. Column chromatography was performed with silica gel (230–400 mesh) following the methods described by Still.[19] Thin layer chromatography (TLC) was performed using silica gel GF254 (0.25 mm thickness). For visualization, the TLC plates were either placed under ultraviolet light or developed with phosphomolybdic acid followed by heating. Air and moisture-sensitive reactions were conducted in flame or oven dried glassware equipped with tightly fitted rubber septa under a positive atmosphere of dry nitrogen. The reagents and solvents were handled using standard syringe techniques. Temperatures above room temperature were maintained using a mineral oil bath heated on a hotplate.

2.1.2 Procedure for the Heck arylation of fumaric acid (1). To a solution of $Pd(OAc)_2$ (5 mol%, 7 mg) in 5 mL of acetic acid were added fumaric acid (**1**) (366 mg, 3.15 mmol) and the 4-methoxyphenyldiazonium tetrafluoroborate salt (140 mg, 0.63 mmol). The mixture was stirred for 2 h at 60 °C and then heating was carried out to 100 °C for 1 h. After that, the solvent was removed under reduced pressure. The residue was purified by flash chromatography (hexane–ethyl acetate 5 : 1) to provide 3-(4-methoxyphenyl)furan-2,5-dione (**3**) as a yellow solid, in 89% yield.

m.p. 141–143 °C.

^{1}H NMR (250 MHz, $CDCl_3$): δ = 3.89 (s, 3H), 6.83 (s, 1H), 7.00 (d, J = 9.0 Hz, 2H), 7.98 (d, J = 9.0 Hz, 2H).

^{13}C NMR (62.5 MHz, $CDCl_3$): δ = 55.6, 114.9, 119.5, 121.0, 131.1, 146.2, 163.3, 164.0, 165.0.

2.1.3 Procedure for the Heck arylation of monoarylated maleic anhydride (3). To a 50 mL round bottomed flask were added POPd (4 mol%, 29.4 mg), sodium acetate (362 mg, 4.41 mmol, 3 equiv.), and monoarylated maleic anhydride (**3**) (300 mg, 1.47 mmol). Acetonitrile (15 mL) was added, followed by the arenediazonium salt (5.88 mmol, 4 equiv.). The reaction was heated at 80 °C for 2 h. After this time, the crude reaction mixture was filtered through a plug of silica gel, and the filtrate was concentrated under reduced pressure. The product was purified by flash chromatography (hexanes–ethyl acetate, 4 : 1) to provide the corresponding Heck adduct.

*3,4-Bis-(4-methoxyphenyl)-furan-2,5-dione (**4a**).* Obtained as a yellow solid, in 89% yield.

^{1}H NMR (500 MHz, $CDCl_3$): δ = 4.06 (s, 6H), 7.50 (d, J = 9.5 Hz, 4H), 8.63 (d, J = 9.5 Hz, 4H).

^{13}C NMR (125 MHz, $CDCl_3$): δ = 55.5, 114.4, 119.9, 131.4, 135.7, 161.7, 165.4.

*3-(4-Methoxyphenyl)-4-(4-hydroxyphenyl)-furan-2,5-dione (**4b**).* Obtained as a yellow solid, in 86% yield.

^{1}H NMR (500 MHz, $CDCl_3$): δ = 3.89 (s, 3H), 5.37 (s, 1H), 6.88 (d, J = 8.5 Hz, 2H), 6.95 (d, J = 8.5 Hz, 2H), 7.55 (d, J = 8.5 Hz, 2H), 7.98 (d, J = 8.5 Hz, 2H).

^{13}C NMR (125 MHz, $CDCl_3$): δ = 55.5, 114.5, 116.0, 119.8, 120.1, 131.5, 131.7, 135.6, 135.9, 157.9, 161.7, 165.53, 165.54.

*3-(4-Methoxyphenyl)-4-(4-methylphenyl)-furan-2,5-dione (**4c**).* Obtained as a yellow solid, in 83% yield.

^{1}H NMR (250 MHz, $CDCl_3$): δ = 2.39 (s, 3H), 3.84 (s, 3H), 6.89 (d, J = 9.0 Hz, 2H), 7.21 (d, J = 8.2 Hz, 2H), 7.46 (d, J = 8.2 Hz, 2H), 7.57 (d, J = 9.0 Hz, 2H).

^{13}C NMR (62.5 MHz, $CDCl_3$): δ = 21.6, 55.4, 114.6, 119.7, 124.8, 129.5, 129.6, 131.6, 135.9, 136.9, 141.4, 161.8, 165.2, 165.3.

*3-(4-Chlorophenyl)-4-(4-methoxyphenyl)-furan-2,5-dione (**4d**).* Obtained as a yellow solid, in 55% yield.

^{1}H NMR (250 MHz, $CDCl_3$): δ = 3.86 (s, 3H), 6.92 (d, J = 8.9 Hz, 2H), 7.40 (d, J = 8.5 Hz, 2H), 7.38–7.57 (m, 4H).

^{13}C NMR (62.5 MHz, $CDCl_3$): δ = 55.5, 114.6, 119.2, 126.1, 129.3, 130.9, 131.7, 134.3, 137.1, 138.1, 162.2, 164.8, 164.9.

2.1.4 Procedure to obtain bisarylated *N*-benzyl maleimides (5a–d). To a microwave test tube were added diaryl maleic anhydride **4a–d** (0.32 mmol), phenol (60 mg, 0.64 mmol), benzylamine (68.6 mg, 0.64 mmol), DIPEA (330.6 mg, 2.56 mmol) and 300 mg of powdered molecular sieves 4 Å. The reaction mixture was stirred in a microwave reactor at 300 W and 110 °C for 1 min, and then kept under these conditions for 2 min. After this time, the crude reaction mixture was diluted in ethyl acetate (9 mL) and washed with HCl 4% solution. The organic layer was dried with $MgSO_4$, filtered, and concentrated under reduced pressure. The residue was purified by flash chromatography (hexane–ethyl acetate, 1.5 : 1) to provide the corresponding bisarylated *N*-benzyl maleimides.

*N-Benzyl-3,4-bis(4-methoxyphenyl)-1H-pyrrole-2,5-dione (**5a**).* Obtained as a yellow solid, in 81% yield.

^{1}H NMR (500 MHz, $CDCl_3$): δ = 3.82 (s, 6H), 4.78 (s, 2H); 6.86 (d, J = 8.8 Hz, 4H), 7.26–7.36 (m, 3H), 7.44–7.50 (m, 6H).

^{13}C NMR (125 MHz, $CDCl_3$): δ = 41.8, 55.3, 114.1, 121.3, 127.7, 128.6, 128.8, 131.4, 134.1, 136.6, 160.7, 171.0.

*N-Benzyl-3-(4-methoxyphenyl)-4-(4-hydroxyphenyl)-1H-pyrrole-2,5-dione (**5b**).* Obtained as a yellow solid, in 65% yield.

^{1}H NMR (250 MHz, DMSO-d6): δ = 3.79 (s, 3H), 4.71 (s, 2H), 6.78 (d, J = 8.8 Hz, 2H), 6.97 (d, J = 8.8 Hz, 2H), 7.27–7.37 (m, 7H), 7.40 (d, J = 8.8 Hz, 2H).

^{13}C NMR (62.5 MHz, DMSO-d6): δ = 41.6, 55.7, 114.65, 115.9, 119.8, 121.6, 129.1, 131.6, 131.8, 133.7, 134.8, 137.4, 137.4, 159.4, 160.6, 171.14, 171.12.

HRMS (ESI$^+$): calcd for $C_{24}H_{19}NO_4/Na^+$ 408.1206; found 408.1201.

*N-Benzyl-3-(4-methoxyphenyl)-4-(4-methylphenyl)-1H-pyrrole-2,5-dione (**5c**).* Obtained as a yellow solid, in 80% yield.

^{1}H NMR (250 MHz, $CDCl_3$): δ = 2.36 (s, 3H), 3.82 (s, 3H), 4.79 (s, 2H), 6.85 (d, J = 8.9 Hz, 2H), 7.15 (d, J = 8.0 Hz, 2H), 7.27–7.44 (m, 9H).

^{13}C NMR (62.5 MHz, $CDCl_3$): δ = 21.5, 41.9, 55.3, 114.0, 121.1, 126.1, 127.8, 128.6, 128.8, 129.3, 129.7, 131.5, 134.4, 135.1, 136.6, 139.9, 160.8, 170.8, 170.9.

HRMS (ESI$^+$): calcd for $C_{25}H_{21}NO_3/Na^+$ 406.1414; found 406.1422.

*N-Benzyl-3-(4-chlorophenyl)-4-(4-methoxyphenyl)-1H-pyrrole-2,5-dione (**5d**).* Obtained as a yellow solid, in 78% yield.

^{1}H NMR (250 MHz, $CDCl_3$): δ = 3.83 (s, 3H), 4.79 (s, 2H), 6.87 (d, J = 8.9 Hz, 2H), 7.31–7.48 (m, 11H).

^{13}C NMR (62.5 MHz, $CDCl_3$): δ = 42.0, 55.3, 114.2, 120.6, 127.5, 127.9, 128.7, 128.8, 128.9, 131.1, 131.6, 132.9, 135.7, 136.2, 136.4, 161.1, 170.4, 170.5.

HRMS (ESI$^+$): calcd for $C_{24}H_{18}ClNO_3/Na^+$ 426.0867; found 426.0873.

2.2 Steady-state absorption and emission measurements

Steady-state experiments were employed to characterize the new fluorophores and to determine their fluorescence quantum yields. Electronic absorption and fluorescence emission measurements were carried out on Jasco V-630 and Hitachi F-4500 spectrometers, respectively. Fluorescence quantum yields (Φ_F) of samples were calculated using 9,10-diphenylanthracene (DPA) (Φ_F = 0.9, cyclohexane) as a standard corrected by refractive index differences.[14] All solvents were of HPLC grade and were dried with 4 Å molecular sieves prior to use. 1,4-Dioxane was previously distilled.

2.3 Time-resolved fluorescence measurements

Fluorescence decays were measured by a time-correlated single-photon counting technique (TCSPC) using a Peltier cooled PMT-MCP (Hamamatsu R3809U-50) as a photon detector. Light pulses at 395 nm were provided by frequency doubling the 150 fs laser pulse of a Ti–Sapphire Mira 900 laser pumped by Verdi 5 W (Coherent). The fluorescence decays were collected in magic angle mode (54.7°) using Glan-Laser polarizers (Newport), with 5×10^3 peak counts and a time increment of 20–100 ps per channel. The typical instrument response function (irf) was 40 ps at FWHM.[11] All analyzed samples had an optical density below 0.5. Decays were recorded with the TC900 counting board and software from Edinburgh Instruments. Lifetimes were evaluated by the reconvolution procedure with multi-exponential decay models, according to eqn (1).

$$I(t) = \sum_i b_i \exp(-t/\tau_i) \tag{1}$$

In eqn (1), τ_i and b_i are the decay time and the pre-exponential factor of the *i*th component, respectively. Decays from compound **5a** were also analyzed by the global analysis method.[14] Global analysis was employed for five wavelengths distributed over the emission band every 15 nm from the emission maximum, using linked-decay times. The decay surfaces were analyzed using the FAST software from Edinburgh Instruments.

2.4 Theoretical calculations

All the structures were optimized before calculations. The Osanger radius, that is the radius of the cavity in which the fluorophore resides,[14] as well as the ground state dipole moment of the compounds were calculated by the density functional theory (DFT) method using the Gaussian 03 software[20] at the B3LYP/6-311G++(2d,2p) level of theory.

3 Results and discussion

3.1 Synthesis of bisarylated maleimides

Maleimides are described in the literature as compounds exhibiting fluorescence,[21,22] and their synthesis is well-documented.[22–24] In 2006, Correia and coworkers[16] developed a direct methodology to obtain bisarylated maleic anhydrides using the Heck arylation with arenediazonium tetrafluoroborates providing symmetrical and unsymmetrical products with better yields. However, to obtain monoarylated maleic anhydrides, an excess of maleic anhydride was necessary.

An improved procedure with fumaric acid (**1**) as the substrate in the Heck–Matsuda reaction, followed by a one-pot cyclization was recently applied (see the reaction scheme of Fig. 1). The use of $Pd(OAc)_2$ in acetic anhydride at 60 °C provides the monoarylated acyclic compound. After the arylation step the reaction system was heated to 100 °C to give the intermediate compound **3** in 89% yield. The bisarylated maleic anhydrides **4a–d** were prepared by a second Heck–Matsuda reaction, using dihydrogen dichlorobis(di-*t*-butylphosphinito-kP)-palladate(II) (POPd) as a pre-catalyst and sodium acetate, in acetonitrile solution for 1 hour, providing good yields. Finally, maleimide compounds were obtained in 65–81% yield with benzylamine, Hünig's base, and phenol at 110 °C, in a microwave (300 W) for 1 minute.

In contrast to the results reported by Mazzanti and coworkers,[25] our diarylmaleimides do not form atropisomers mainly because compounds **5a–d** lack *ortho* substituents. The absence of *ortho* substituents causes an easy and fast equilibration between the isomers. This aspect of our fluorophores is also confirmed from the ^{1}H and ^{13}C NMR spectra of the compounds, which show no signals of rotamers but only a sharp signal appearing for the methoxy/methyl groups. The conformation (optimized geometry) and the dipole moments for the biarylmaleimides **5a–d** can be found in the ESI.†

3.2 Photophysics of bisarylated maleimides

3.2.1 Steady-state experiments. Electronic absorption spectra of the compounds exhibited single non-structured bands centered from 390 nm with no relevant effects below 300 nm. However, for solvents like diethyl ether and di-*n*-propyl ether, we can observe an absorption band around 230 nm. Similar absorption band profiles were found for bisindolylmaleimides.[26,27] The absorption spectra showed negligible changes with solvent polarity. These spectra can be found in the ESI.† All maleimide derivatives presented broad fluorescence emission bands in the visible range, with emission peaks between 550 and 568 nm.

It is known that upon adding electron donating groups to aromatic compounds, an increase in the maximum wavelengths of absorption and emission is expected. This behavior was observed for these maleimides and is in good agreement with the results of Xie *et al.*,[28] in which semi-empirical quantum chemical calculations were used to predict the maximum wavelength of absorption and emission spectra of some similar compounds.

The fluorescence emissions had a notable solvatochromic effect at about 960 cm^{-1}, and the calculated Stokes shifts are within the range of 6075–7292 cm^{-1}, a strong indicator that the dipole moment of these dyes in the excited state is higher than the corresponding value in the ground state. For instance, a typical positive solvatochromic shift of compound **5a** is illustrated in Fig. 2 and its spectral parameters with increasing solvent polarity are summarized in Table 1. These results can be ascribed to a push–pull effect, in which a significant charge shift occurs.[12] The behavior of typical push–pull chromophors, like merocyanines, cyanostilbenes[12] and *p*-dimethylamino-4-nitrostilbene (DMANS),[13] is in good agreement with the data reported here.

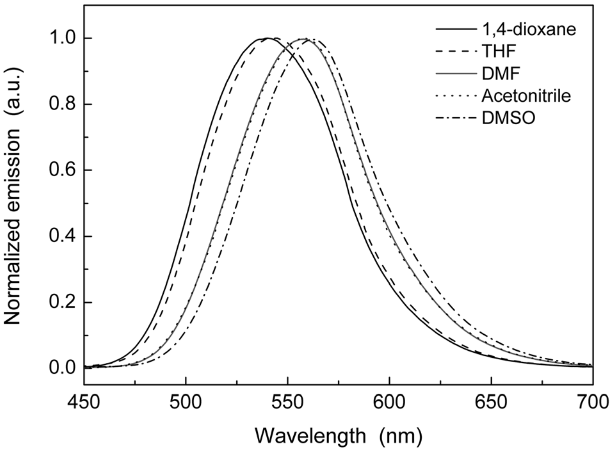

Fig. 2 Solvatochromic shift in emission spectra of **5a**.

In general, the largest Stokes shift was observed in acetonitrile and the lowest in THF. The fluorescence quantum yields are higher in nonpolar solvents like 1,4-dioxane and THF (values between 0.24 and 0.71), indicating that solvent deactivation of the excited state is less effective in nonpolar media. The same trends were found for triarylamine compounds.[29]

The increase in solvent polarity from 1,4-dioxane to DMSO resulted in a red shift of the emission of compound **5a** at about 757 cm^{-1}, because of the solvent stabilization of the excited state.[30,31] Moreover, compounds **5b**, **5c**, and **5d** followed the same trend in emission as that observed for compound **5a**.

The lowest Stokes shift was observed in **5b** that has a 4-hydroxyphenyl group. In such a compound a solvent assisted proton transfer process may take place. This process should decrease the fluorescence quantum yield because the excited state phenolate formed may have low emission efficiency, and this behavior was barely observed in steady-state emission measurements (quantum yield values between 0.04 and 0.38). On the other hand, **5d** exhibited the highest emission quantum yield (0.71) compared to **5b** (0.24) in 1,4-dioxane. This fact may be related to the effect of substitution of OH by Cl in position 4 of the phenyl substituent, precluding further the solvent assisted proton transfer process.

The bisarylmaleimides presented here are in good agreement with bisindolylmaleimide systems. In both cases, a substantial, but not complete, charge shift in the excited state takes place.[26,27,32–35]

The issues raised here about the photophysics of the bisarylated maleimides from the analysis of the steady-state emission properties will in part be supported by the time-resolved fluorescence behavior found in different solvents.

3.2.2 Time-resolved experiments. Time-resolved experiments are crucial to characterize new fluorophores and to investigate dynamic processes in the singlet excited state. The global analysis of the fluorescence decay surface of compound **5a** reveals short lived components in the range of 1.34–7.55 ns and long lived components in the narrow range of 11.52–13.55 ns with a biexponential fitting in polar solvents. However, in nonpolar solvents like 1,4-dioxane and THF the decays are single exponential and lifetimes are very close to values of long lived components observed in the polar solvents.

The maleimides present two dipolar Lewis structures, which contribute to a single excited species. The combination of similar spectral behavior in different solvents and linear Lippert–Mataga plots (see below) suggests that the emission is due to the same dipolar species in all solvents. Therefore, we can infer that the long decay corresponds to emission from the charge shift or the push–pull state. The time-resolved para-

Table 1 Steady-state data of maleimides

Compound		Solvent	λ_{abs} [a] (nm)	λ_{em} [b] (nm)	E_{0-0} [c] (eV)	$\Delta\nu$ [d] (cm^{-1})	Φ_F [e]
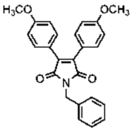	**5a**	1,4-Dioxane	402	540	2.60	6954	0.39
		THF	406	544	2.59	6248	0.43
		DMSO	406	563	2.52	6869	0.24
		DMF	404	556	2.54	6767	0.27
		Acetonitrile	400	558	2.57	7079	0.24
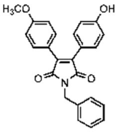	**5b**	1,4-Dioxane	404	540	2.59	6234	0.24
		THF	410	546	2.57	6075	0.38
		DMSO	413	568	2.49	6607	0.04
		DMF	411	564	2.51	6600	0.11
		Acetonitrile	401	558	2.56	7017	0.23
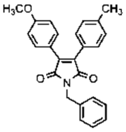	**5c**	1,4-Dioxane	393	526	2.68	6434	0.32
		THF	394	526	2.66	6369	0.53
		DMSO	396	554	2.59	7202	0.34
		DMF	394	545	2.61	7032	0.36
		Acetonitrile	390	545	2.66	7292	0.35
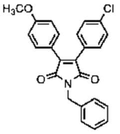	**5d**	1,4-Dioxane	392	526	2.68	6499	0.71
		THF	394	529	2.67	6477	0.35
		DMSO	394	550	2.60	7199	0.24
		DMF	392	548	2.62	7262	0.36
		Acetonitrile	389	543	2.66	7291	0.39

[a] Maximum absorption wavelength. [b] Maximum emission wavelength. [c] Energy of transition 0–0. [d] Stokes shift. [e] Fluorescence quantum yield.

meters are summarized in Table 2 and typical fluorescence decays are depicted in Fig. 3. The values of E_{0-0} presented in Table 1 support partially this assumption and a small decrease of energy level with solvent polarity is observed.

The fluorescence of compound **5c** followed a similar trend to that observed for compound **5a**, but only for 1,4-dioxane a single exponential behavior was found. In the other solvents the fluorescence decays were of biexponential character. This biexponential behavior may be ascribed to a specific interaction of the excited state with the charge shift or push–pull character with the electron donating solvents, and the short component in a low weight percent would correspond to decay of a weak solvent complex, as observed by Chandross and coworkers for intramolecular exciplex systems.[36] For compound **5d**, the presence of the electron withdrawing 4-chlorophenyl group gives no difference in dynamic and spectral fluorescence properties when compared with compounds **5a** and **5c**. It seems to indicate that a single branch charge shift from the 4-methoxy donor group to the carbonyl acceptor is operating in the charge shift process, and the presence of the second aryl substituted branch with the 4-chlorophenyl group takes no effect in the whole charge shift.

Table 2 Time-resolved data of maleimides

Compound	Solvent	τ_1 (ns)	τ_2 (ns)	b_1 [a]	b_2	χ^2 [b]
5a	1,4-Dioxane	—	13.79	—	1.00	1.05
	THF	—	13.52	—	1.00	1.07
	DMSO	2.18	11.52	0.17	0.83	1.09
	DMF	7.55	13.45	0.24	0.76	1.07
	Acetonitrile	1.34	13.55	0.08	0.92	1.07
5b	1,4-Dioxane	—	12.86	—	1.00	1.05
	THF	—	12.01	—	1.00	1.05
	DMSO	0.83	2.65	0.11	0.89	1.12
	DMF	0.99	3.28	0.11	0.89	1.14
	Acetonitrile	—	11.48	—	1.00	1.12
5c	1,4-Dioxane	—	13.88	—	1.00	1.11
	THF	3.77	13.66	0.08	0.92	1.00
	DMSO	7.20	11.97	0.24	0.76	1.17
	DMF	5.58	12.67	0.07	0.93	1.18
	Acetonitrile	1.44	13.75	0.05	0.95	1.12
5d	1,4-Dioxane	—	12.39	—	1.00	1.05
	THF	—	11.55	—	1.00	1.07
	DMSO	5.22	8.62	0.25	0.75	1.23
	DMF	—	10.51	—	1.00	1.19
	Acetonitrile	1.77	12.00	0.06	0.94	1.11

[a] $b_i = B_i/\sum B_i$, B_i is the pre-exponential factor in the model function for exponential component analysis. [b] χ^2 = the chi-square value of the decay fitting. For **5a**, it corresponds to χ^2_g, the global decay fitting.

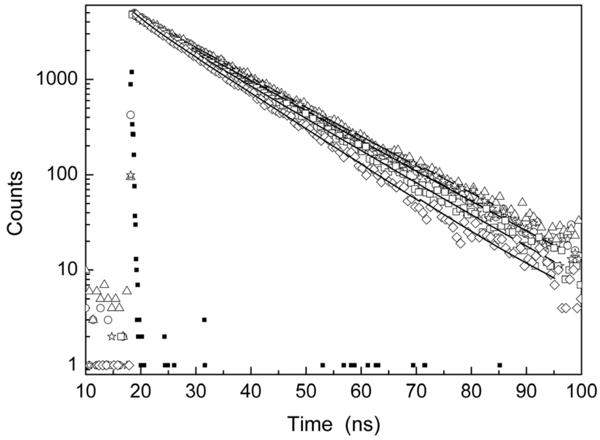

Fig. 3 Fluorescence decays of compound **5a** in: 1,4-dioxane (△) λ_{em} = 540 nm; THF (☆) λ_{em} = 544 nm; DMSO (◊) λ_{em} = 563 nm; DMF (□) λ_{em} = 556 nm; acetonitrile (○) λ_{em} = 558 nm; (■) irf. λ_{exc} = 395 nm.

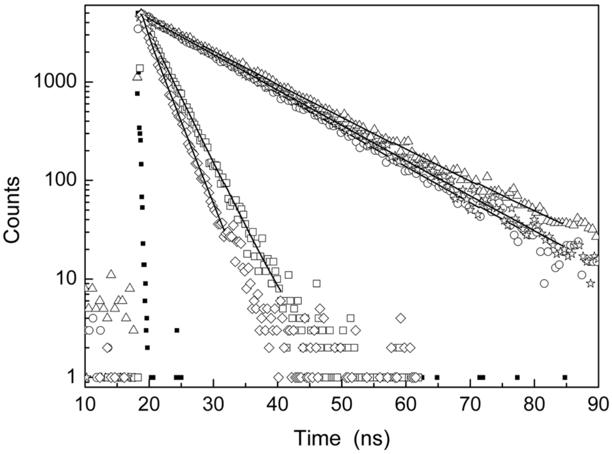

Fig. 4 Fluorescence decays of compound **5b** in: 1,4-dioxane (△) λ_{em} = 540 nm; THF (☆) λ_{em} = 549 nm; DMSO (◊) λ_{em} = 568 nm; DMF (□) λ_{em} = 564 nm; acetonitrile (○) λ_{em} = 558 nm; (■) irf. λ_{exc} = 395 nm.

Most notable is the excited state dynamics of **5b** in DMSO and in DMF. It exhibited biexponential decays with a very short component of less than 1 ns as illustrated in Fig. 4.

This hydroxyl-substituted derivative may deprotonate in polar solvents with the proton accepting character like DMF and DMSO, thus emission from the corresponding phenolate ion may occur. The value of the second decay component of compound **5b** in DMF and DMSO is in agreement with the fluorescence lifetime of phenolate anions.[37] For compound **5b** in 1,4-dioxane, THF, and acetonitrile the decays are of single exponential character, which indicates that an excited state charge transfer process does not occur, precluding further proton transfer mediated by solvent interactions.

Considering that a solvent assisted excited state proton transfer may play a role for this compound, if one uses **5a** as a model compound, the comparison of it with **5b** allows the rate constant of proton transfer (k_{pt}) to be evaluated. In the approximation of the very fast excited state intramolecular charge shift process:

$$k_{\mathrm{pt}} = (1/\tau_1)_{\mathbf{5b}} - (1/\tau_1)_{\mathbf{5a}} \tag{2}$$

Using eqn (2), the values of k_{pt} in DMF and DMSO are 0.9×10^9 and 1.3×10^9 s^{-1}, respectively. This result indicates that the deactivation rate of the excited state *via* deprotonation occurs at a rate similar to that observed in solvent assisted proton transfer processes studied by Kasha and coworkers.[38]

3.3 Dipole moment analysis

Fluorophores exhibiting the solvatochromic shift are valuable probes to monitor the micropolarity in their surrounding environment.[39,40] This effect may be studied by the Lippert–Mataga approach[17,18] that correlates the effect of solvent polarity on the Stokes shift with the difference in dipole moments[14,15] by

$$\nu_{\mathrm{A}} - \nu_{\mathrm{F}} = \frac{2}{hca^3}\Delta f(\mu_{\mathrm{E}} - \mu_{\mathrm{G}})^2 + C \tag{3}$$

$$\Delta f = \frac{\varepsilon - 1}{2\varepsilon + 1} - \frac{n^2 - 1}{2n^2 + 1} \tag{4}$$

In eqn (3), ν_A–ν_F is the Stokes shift (cm^{-1}), a is the radius of the Osanger cavity, h is Planck's constant, c is the speed of light, C is a constant, and μ_E and μ_G are the excited and ground state dipole moments, respectively. In eqn (4), Δf is a parameter called orientation polarizability, which is calculated from the dielectric constant ε and the refractive index n of the solvent.

A typical Lippert–Mataga plot for compound **5a** is depicted in Fig. 5. The plot was obtained based on the emission maxima. Using eqn (3) a positive slope of 6681 cm^{-1} is obtained. For the other compounds, reasonable linear fits were obtained indicating no existence of strong specific solvent effects (see in ESI†). From the calculated dipole moment difference, according to eqn (3), and using the values of the dipole moment in the ground state and Osanger cavities evaluated from DFT quantum chemical calculations, the excited state dipole moments of the maleimides were obtained and the values found are reported in Table 3.

In general, the differences in dipole moment in ground and excited states of the compounds are within a narrow range of 11–13 D, indicating a similar contribution of a charge shift process in the excited states.[41,42] In the case of compound **5b** no good correlation in the Lippert–Mataga plot was observed,

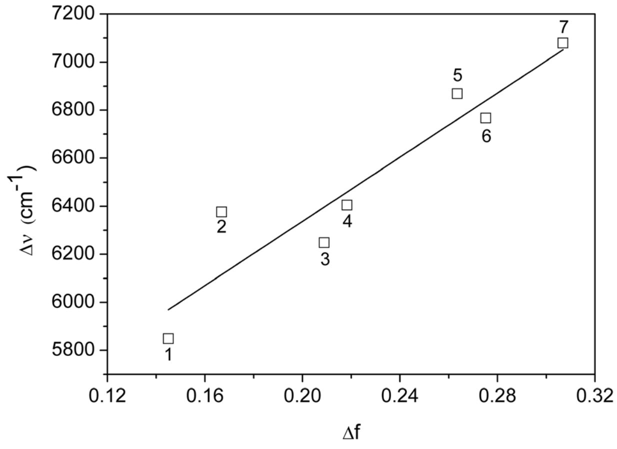

Fig. 5 Lippert–Mataga plot of compound **5a** according to eqn (3). 1: di-*n*-propyl ether, 2: diethyl ether, 3: THF, 4: CH_2Cl_2, 5: DMSO, 6: DMF, 7: acetonitrile.

Table 3 Theoretical parameters and the calculated excited state dipole moment (μ_E)

Compound	a_0 (Å)[a]	μ_G (D)[b]	$\Delta\mu$ (D)[c]	μ_E (D)[d]
5a	6.0	4.3	11.9	16.2
5c	5.9	4.2	12.5	16.7
5d	5.7	3.0	12.6	15.6

[a] a_0 = the radius of the Onsager cavity. [b] μ_G = the ground state dipole moment. [c] $\Delta\mu$ = variation of dipole moments. [d] μ_E = the excited state dipole moment.

probably due to the deprotonation process in polar solvents as previously discussed.

4 Conclusions

In summary, four maleimides based on natural products were synthesized by the Heck reaction. The fluorescence properties of these new bisarylated maleimide derivatives are modeled by solvent and substituent effects. The compounds showed a positive solvatochromic shift and a substantial charge shift process. The difference in dipole moment between ground and excited states of about 12 D corroborates this conclusion.

Acknowledgements

The authors thank G. R. Nagurniak and A. B. F. da Silva, from the Quantum Chemistry Group of IQSC – USP, for providing quantum chemical data. Financial support was provided by FAPESP (grants 2011/18215-8 and 2011/23832-6), CNPq, and CAPES Brazilian research funds. M. H. Lauer thanks FAPESP for the doctoral scholarship 2011/08727-1. R. L. Drekener thanks FAPESP for the post-doctoral fellowship 2010/12193-0.

Notes and references

1 M. D. Alexander, M. D. Burkart, M. S. Leonard, P. Portonovo, B. Liang, X. B. Ding, M. M. Joullie, B. M. Gulledge, J. B. Aggen, A. R. Chamberlin, J. Sandler, W. Fenical, J. Cui, S. J. Gharpure, A. Polosukhin, H. R. Zhang, P. A. Evans, A. D. Richardson, M. K. Harper, C. M. Ireland, B. G. Vong, T. P. Brady, E. A. Theodorakis and J. J. La Clair, A central strategy for converting natural products into fluorescent probes, *ChemBioChem*, 2006, **7**, 409–416.

2 J. S. Sandler, W. Fenical, B. M. Gulledge, A. R. Chamberlin and J. J. La Clair, Fluorescent profiling of natural product producers, *J. Am. Chem. Soc.*, 2005, **127**, 9320–9321.

3 F. Hentschel, F. Sasse and T. Lindel, Fluorescent analogs of the marine natural product psammaplin A: synthesis and biological activity, *Org. Biomol. Chem.*, 2012, **10**, 7120–7133.

4 S. Manning, W. Bogen and L. Kelly, Synthesis, characterization, and photophysical study of fluorescent *N*-substituted benzo[ghi]perylene "swallow tail" monoimides, *J. Org. Chem.*, 2011, **76**, 6007–6013.

5 M. J. Dalton, R. Kannan, J. E. Haley, G. S. He, D. G. McLean, T. M. Cooper, P. N. Prasad and L.-S. Tan, Aromatic polyimides containing main-chain diphenylamino-fluorene-benzothiazole motif: fluorescence quenching, two-photon properties, and exciplex formation in a solid state, *Macromolecules*, 2011, **44**, 7194–7206.

6 A. Rudi, I. Goldberg, Z. Stein, F. Frolow, Y. Benayahu, M. Schleyer and Y. Kashman, Polycitone A and polycitrin-A and polycitrin-B. New alkaloids from the marine ascidian *Polycitor* sp, *J. Org. Chem.*, 1994, **59**, 999–1003.

7 Y. Suzuki and K. Yokoyama, Design and synthesis of intramolecular charge transfer-based fluorescent reagents for the highly-sensitive detection of proteins, *J. Am. Chem. Soc.*, 2005, **127**, 17799–17802.

8 K. Kudo, A. Momotake, J. K. Tanaka, Y. Miwa and T. Arai, Environmental polarity estimation in living cells by use of quinoxaline-based full-colored solvatochromic fluorophore PQX and its derivatives, *Photochem. Photobiol. Sci.*, 2012, **11**, 674–678.

9 R. V. Pereira and M. H. Gehlen, Polymerization and conformational transition of poly(methacrylic acid) probed by electronic spectroscopy of aminoacridines, *Macromolecules*, 2007, **40**, 2219–2223.

10 B. M. Sheikhali and R. G. Weiss, Effects of aggregation and mesomorphic order on the photophysical properties of 4-alkyl-*N*-(*p*-cyanophenyl)piperidines. Molecules capable of forming intramolecular charge-transfer states, *J. Am. Chem. Soc.*, 1994, **116**, 6111–6120.

11 A. P. Garcia Ferreira, R. Frederice, K. P. F. Janssen and M. H. Gehlen, Dually fluorescent silica nanoparticles, *J. Lumin.*, 2011, **131**, 888–893.

12 P. D. Zoon and A. M. Brouwer, A push-pull aromatic chromophore with a touch of merocyanine, *Photochem. Photobiol. Sci.*, 2009, **8**, 345–353.

13 I. D. Petsalakis, D. G. Georgiadou, M. Vasilopoulou, G. Pistolis, D. Dimotikali, P. Argitis and G. Theodorakopoulos, Theoretical Investigation on the Effect of Protonation on the Absorption and Emission Spectra of Two Amine-Group-Bearing, Red "Push-Pull" Emitters, 4-Dimethylamino-4′-nitrostilbene and 4-(dicyanomethylene)-2-methyl-6-*p*-(dimethylamino)styryl-4*H*-pyran, by DFT and TDDFT Calculations, *J. Phys. Chem. A*, 2010, **114**, 5580–5587.

14 J. R. Lakowicz, *Principles of fluorescence spectroscopy*, Springer, New York, 2006.

15 Z. R. Grabowski, K. Rotkiewicz and W. Rettig, Structural changes accompanying intramolecular electron transfer: Focus on twisted intramolecular charge-transfer states and structures, *Chem. Rev.*, 2003, **103**, 3899–4031.

16 (*a*) A. C. B. Burtoloso, A. L. L. Garcia, K. C. Miranda and C. R. D. Correia, Heck arylation of maleic anhydrides using arenediazonium tetrafluoroborates: Synthesis of mono- and diarylated maleic anhydrides and of the marine alkaloids prepolycitrin A and polycitrin A, *Synlett*, 2006, 3145–3149; (*b*) K. Canto, R. S. Ribeiro, A. F. P. Biajoli and C. R. D. Correia, Expeditious Synthesis of the Marine Natural Products Prepolycitrin A and Polycitrins A and B through Heck Arylations, *Eur. J. Org. Chem.*, 2013, 8004–8013.

17 E. V. Lippert, Spektroscopische bistimmung des dipolmomentes aromatischer verbindungen im ersten angeregten singulettzustand, *Z. Electrochem.*, 1957, **61**, 962–975.

18 N. Mataga, Y. Kaifu and M. Koizumi, Solvent effects upon fluorescence spectra and the dipole moments of excited molecules, *Bull. Chem. Soc. Jpn.*, 1956, **29**, 465–470.

19 W. C. Still, M. Kahn and A. Mitra, Rapid chromatographic technique for preparative separations with moderate resolution, *J. Org. Chem.*, 1978, **43**, 2923–2925.

20 M. J. Frisch, G. W. Trucks, H. B. Schlegel, G. E. Scuseria, M. A. Robb, J. R. Cheeseman, J. A. Montgomery, Jr., T. Vreven, K. N. Kudin, J. C. Burant, J. M. Millam, S. S. Iyengar, J. Tomasi, V. Barone, B. Mennucci, M. Cossi, G. Scalmani, N. Rega, G. A. Petersson, H. Nakatsuji, M. Hada, M. Ehara, K. Toyota, R. Fukuda, J. Hasegawa, M. Ishida, T. Nakajima, Y. Honda, O. Kitao, H. Nakai, M. Klene, X. Li, J. E. Knox, H. P. Hratchian, J. B. Cross, V. Bakken, C. Adamo, J. Jaramillo, R. Gomperts, R. E. Stratmann, O. Yazyev, A. J. Austin, R. Cammi, C. Pomelli, J. W. Ochterski, P. Y. Ayala, K. Morokuma, G. A. Voth, P. Salvador, J. J. Dannenberg, V. G. Zakrzewski, S. Dapprich, A. D. Daniels, M. C. Strain, O. Farkas, D. K. Malick, A. D. Rabuck, K. Raghavachari, J. B. Foresman, J. V. Ortiz, Q. Cui, A. G. Baboul, S. Clifford, J. Cioslowski, B. B. Stefanov, G. Liu, A. Liashenko, P. Piskorz, I. Komaromi, R. L. Martin, D. J. Fox, T. Keith, M. A. Al-Laham, C. Y. Peng, A. Nanayakkara, M. Challacombe, P. M. W. Gill, B. Johnson, W. Chen, M. W. Wong, C. Gonzalez and J. A. Pople, Gaussian Inc., Wallingford CT, 2004.

21 H. C. Yeh, W. C. Wu and C. T. Chen, The colourful fluorescence from readily-synthesized 3,4-diaryl-substituted maleimide fluorophores, *Chem. Commun.*, 2003, 404–405.

22 E. K. Fields, S. J. Behrend, S. Meyerson, M. L. Winzenburg, B. R. Ortega and H. K. Hall, Diaryl-substituted maleic anhydrides, *J. Org. Chem.*, 1990, **55**, 5165–5170.

23 W. D. Dean and D. M. Blum, Condensation of arylacetonitriles with glyoxylic-acid. Facile synthesis of arylmaleic acid-derivatives, *J. Org. Chem.*, 1993, **58**, 7916–7917.

24 M. S. Newman and W. M. Stalick, Novel synthesis of disubstituted maleic anhydrides by pyrolysis of 1-ethoxy-1-alkenyl esters of alpha-keto acids, *J. Org. Chem.*, 1973, **38**, 3386–3389.

25 M. Ambrogi, A. Ciogli, M. Mancinelli, S. Ranieri and A. Mazzanti, Atropisomers of Arylmaleimides: Stereodynamics and Absolute Configuration, *J. Org. Chem.*, 2013, **78**, 3709–3719.

26 B. K. Kaletas, R. M. Williams, B. Konig and L. De Cola, Strong fluorescence enhancement of 2-bromo-3-(1*H*-indol-3-yl)maleimide upon coordination to a Lewis-acidic metal complex, *Chem. Commun.*, 2002, 776–777.

27 B. K. Kaletas, H. C. Joshi, G. van der Zwan, M. Fanti, F. Zerbetto, K. Goubitz, L. De Cola, B. Konig and R. A. Williams, Asymmetric Indolylmaleimide Derivatives and Their Complexation with Zinc(II)-Cyclen, *J. Phys. Chem. A*, 2005, **109**, 9443–9455.

28 H.-d. Xie, L. A. Ho, M. S. Truelove, B. Corry and S. G. Stewart, Fluorescent Triphenyl Substituted Maleimide Derivatives: Synthesis, Spectroscopy and Quantum Chemical Calculations, *J. Fluoresc.*, 2010, **20**, 1077–1085.

29 J. M. Chudomel, B. Yang, M. D. Barnes, M. Achermann, J. T. Mague and P. M. Lahti, Highly twisted triarylamines for photoinduced intramolecular charge transfer, *J. Phys. Chem. A*, 2011, **115**, 8361–8368.

30 R. V. Pereira, A. P. G. Ferreira and M. H. Gehlen, Excited-state intramolecular charge transfer in 9-aminoacridine derivative, *J. Phys. Chem. A*, 2005, **109**, 5978–5983.

31 K. Guzow, M. Czerwinska, A. Ceszlak, M. Kozarzewska, M. Szabelski, C. Czaplewski, A. Lukaszewicz, A. A. Kubicki and W. Wiczk, Photophysical properties of 3-[2-(*N*-phenylcarbazolyl)-benzoxazol-5-yl]alanine derivatives – experimental and theoretical studies, *Photochem. Photobiol. Sci.*, 2013, **12**, 284–297.

32 B. K. Kaletas, C. Mandl, G. van der Zwan, M. Fanti, F. Zerbetto, L. De Cola, B. Konig and R. M. Williams, Unexpected Photophysical Properties of Symmetric Indolylmaleimide Derivatives, *J. Phys. Chem. A*, 2005, **109**, 6440–6449.

33 E. M. Kosower and J. R. De Souza, $n\pi$-ct-π^* Transitions: $n\pi^*$ Transitions of the second kind, *Chem. Phys.*, 2006, **324**, 3–7.

34 M. Nakazono, A. Jinguji, S. Nanbu, R. Kuwano, Z. Zheng, K. Saita, Y. Oshikawa, Y. Mikuni, T. Murakami, Y. Zhao, S. Sasaki and K. Zaitsu, Fluorescence and chemiluminescence properties of indolylmaleimides: experimental and theoretical studies, *Phys. Chem. Chem. Phys.*, 2010, **12**, 9783–9793.

35 Z. Zheng, Y. Zhao, M. Nakazono and S. Nanbu, Theoretical study of photo-physical properties of indolylmaleimide derivatives, *Phys. Chem. Chem. Phys.*, 2012, **14**, 3017–3024.

36 E. A. Chandross and H. T. Thomas, The interaction between aminehydrocarbon exciplexes with small dipolar molecules – Stoichiometric complex formation, *Chem. Phys. Lett.*, 1971, **9**, 397–400.

37 R. Das, S. Mitra and S. Mukherjee, Proton-transfer and anion formation in the ground and excited-states of 4-methyl-2,6-diformyl phenol in highly polar aprotic-solvents, *J. Photochem. Photobiol., A*, 1993, **76**, 33–38.

38 M. Kasha, Proton-transfer spectroscopy - Perturbation of the tautomerization potential, *J. Chem. Soc., Faraday Trans. 2*, 1986, **82**, 2379–2392.

39 A. J. Carmichael and K. R. Seddon, Polarity study of some 1-alkyl-3-methylimidazolium ambient-temperature ionic liquids with the solvatochromic dye, Nile Red, *J. Phys. Org. Chem.*, 2000, **13**, 591–595.

40 S. Feryforgues, J. P. Fayet and A. Lopez, Drastic changes in the fluorescence properties of NBD probes with the polarity of the medium: involvement of a TICT state?, *J. Photochem. Photobiol., A*, 1993, **70**, 229–243.

41 R. V. Pereira and M. H. Gehlen, Picosecond fluorescence dynamics of auramine with a long aliphatic chain, *Chem. Phys. Lett.*, 2006, **417**, 425–429.

42 E. Oliveira, R. M. F. Baptista, S. P. G. Costa, M. M. M. Raposo and C. Lodeiro, Synthesis and solvatochromism studies of novel bis(indolyl)methanes bearing functionalized arylthiophene groups as new colored materials, *Photochem. Photobiol. Sci.*, 2014, **13**, 492–498.